Since January 2020 Elsevier has created a COVID-19 resource centre with free information in English and Mandarin on the novel coronavirus COVID-19. The COVID-19 resource centre is hosted on Elsevier Connect, the company's public news and information website.

Research Article
Viral Hepatitis

JOURNAL
OF HEPATOLOGY

SARS-CoV-2 infection of the liver directly contributes to hepatic impairment in patients with COVID-19

Graphical abstract

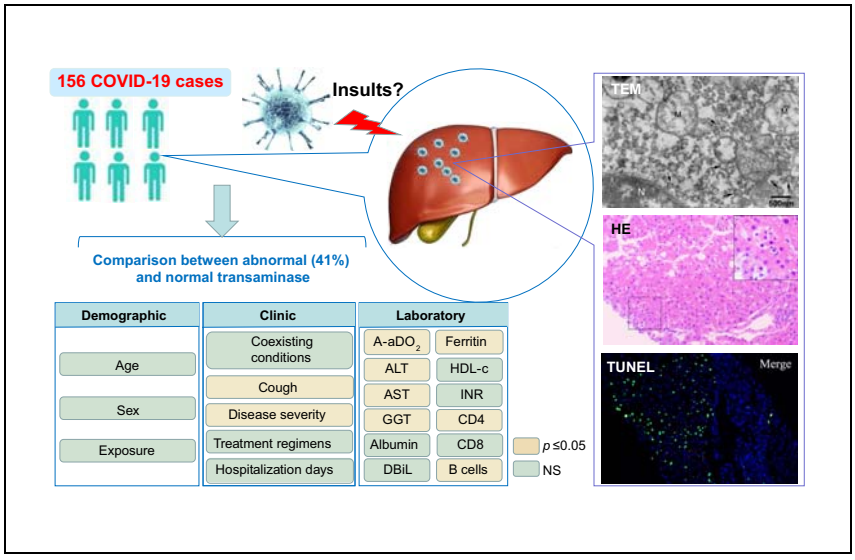

Highlights

- Liver enzyme abnormalities in patients with COVID-19 are associated with disease severity.
- Patients with liver enzyme abnormalities have higher A-aDO2 and GGT, lower albumin and decreased circulating CD4+ T cells and B lymphocytes.
- SARS-CoV-2 is able to infect the liver and cause conspicuous hepatic cytopathy.
- Massive apoptosis and binuclear hepatocytes were the predominant histological features of SARS-CoV-2-infected liver.

Authors

Yijin Wang, Shuhong Liu, Hongyang Liu, …, Shousong Zhao, Jiangyang Lu, Jingmin Zhao

Correspondence

jmzhao302@163.com (J. Zhao).

Lay summary

Liver enzyme abnormalities are common in patients with coronavirus disease 2019 (COVID-19). We reported the clinical characteristics and liver pathological manifestations of COVID-19 patients with elevated liver enzymes. Our findings suggested that SARS-CoV-2 infection of the liver is a crucial factor contributing to hepatic impairment in patients with COVID-19.

https://doi.org/10.1016/j.jhep.2020.05.002

Research Article
Viral Hepatitis

JOURNAL OF HEPATOLOGY

SARS-CoV-2 infection of the liver directly contributes to hepatic impairment in patients with COVID-19

Yijin Wang[1,#], Shuhong Liu[1,#], Hongyang Liu[1,#], Wei Li[2,#], Fang Lin[3], Lina Jiang[1], Xi Li[1], Pengfei Xu[1], Lixin Zhang[1], Lihua Zhao[1], Yun Cao[2], Jiarui Kang[4], Jianfa Yang[1], Ling Li[1], Xiaoyan Liu[1], Yan Li[1], Ruifang Nie[1], Jinsong Mu[3], Fengmin Lu[5], Shousong Zhao[2], Jiangyang Lu[4], Jingmin Zhao[1,*]

[1]*Department of Pathology and Hepatology, The Fifth Medical Center of Chinese PLA General Hospital, Beijing, China;* [2]*Department of Infectious Diseases, The First Affiliated Hospital of Bengbu Medical College, Bengbu, China;* [3]*Department of Intensive Care Unit, The Fifth Medical Center of Chinese PLA General Hospital, Beijing, China;* [4]*Department of Pathology, The Fourth Medical Center of Chinese PLA General Hospital, Beijing, China;* [5]*Department of Microbiology and Infectious Disease Center, School of Basic Medical Sciences, Peking University Health Science Center, Beijing, China*

Background & Aims: Liver enzyme abnormalities are common in patients with coronavirus disease 2019 (COVID-19). Whether or not severe acute respiratory syndrome coronavirus 2 (SARS-CoV-2) infection can lead to liver damage *per se* remains unknown. Herein, we reported the clinical characteristics and liver pathological manifestations of COVID-19 patients with liver enzyme abnormalities.

Methods: We analyzed 156 patients diagnosed with COVID-19 from 2 designated centers in China and compared clinical features between patients with or without elevated aminotransferases. Postmortem liver biopsies were obtained from 2 cases who had elevated aminotransferases. We investigated the patterns of liver impairment by electron microscopy, immunohistochemistry, TUNEL assay and pathological studies.

Results: Sixty-four out of 156 (41.0%) patients with COVID-19 had elevated aminotransferases. The median levels of alanine aminotransferase were 50 U/L *vs.* 19 U/L, respectively, aspartate aminotransferase were 45.5 U/L *vs.* 24 U/L, respectively in abnormal and normal aminotransferase groups. Liver enzyme abnormalities were associated with disease severity, as well as a series of laboratory tests including higher alveolar-arterial oxygen partial pressure difference, higher gamma-glutamyltransferase, lower albumin, decreased CD4+ T cells and B lymphocytes. Ultrastructural examination identified typical coronavirus particles, characterized by spike structures, in the cytoplasm of hepatocytes in 2 COVID-19 cases. SARS-CoV-2-infected hepatocytes displayed conspicuous mitochondrial swelling, endoplasmic reticulum dilatation and glycogen granule decrease. Histologically, massive hepatic apoptosis and some binuclear hepatocytes were observed. Taken together, both ultrastructural and histological evidence indicated a typical lesion of viral infection. Immunohistochemical results showed scarce CD4+ and CD8+ lymphocytes. No obvious eosinophil infiltration, cholestasis, fibrin deposition, granuloma, massive central necrosis, or interface hepatitis were observed.

Conclusions: SARS-CoV-2 infection in the liver directly contributes to hepatic impairment in patients with COVID-19. Hence, a surveillance of viral clearance in liver and long-term outcome of COVID-19 is required.

Lay summary: Liver enzyme abnormalities are common in patients with coronavirus disease 2019 (COVID-19). We reported the clinical characteristics and liver pathological manifestations of COVID-19 patients with elevated liver enzymes. Our findings suggested that SARS-CoV-2 infection of the liver is a crucial factor contributing to hepatic impairment in patients with COVID-19.

Introduction

Coronavirus disease 2019 (COVID-19) caused by severe acute respiratory syndrome coronavirus 2 (SARS-CoV-2) has spread globally, resulting in an ongoing pandemic. The epidemic outbreak of SARS-CoV-2 has caused more than 1.7 million confirmed infections and over 100 thousand fatal cases by April 11th, 2020, affecting 210 countries. Genetically, deep sequencing of lower respiratory tract samples characterizes the virus as a distinct clade from the betacoronaviruses associated with human severe acute respiratory syndrome coronavirus (SARS-CoV) and Middle East respiratory syndrome coronavirus.[1,2] The full spectrum of COVID-19 ranges from mild, self-limiting respiratory tract illness to severe progressive pneumonia. The common clinical manifestations of COVID-19 include elevated body temperature, dry cough, dyspnea, and no obvious improvement after 3 days of antibiotic treatment, as well as white blood cells (WBC) decreasing and pulmonary infiltrate. However, liver enzyme abnormalities are the most striking additional feature observed in these patients. These abnormalities have been reported in up to 50% of patients with COVID-19 and raise great clinical concern,[3–5] despite SARS-CoV-2 being considered a pneumophila virus. Whether or not the cytopathy of hepatocytes elicited

Keywords: COVID-19; Liver enzyme abnormality; Transaminase; SARS-CoV-2 infection; Cytopathy.
Received 13 March 2020; received in revised form 27 April 2020; accepted 3 May 2020; available online 11 May 2020

* Corresponding author. Address: Department of Pathology and Hepatology, The Fifth Medical Center of Chinese PLA General Hospital, No. 100 Xi Si Huan Middle Road, Beijing 100039, China.
E-mail address: jmzhao302@163.com (J. Zhao).
[#] Contributed equally to this article.

https://doi.org/10.1016/j.jhep.2020.05.002

by SARS-CoV-2 infection causes the liver impairment remains unknown.

In this study, we received 156 patients with COVID-19 from 2 designated centers and compared clinical features between abnormal and normal liver enzyme groups. Importantly, through histological, ultrastructural and immunohistochemical examinations on biopsied liver tissues, we found that direct SARS-CoV-2 infection of liver cells significantly contributes to hepatic impairment in patients with COVID-19.

Patients and methods

Patients and study design

We reviewed the medical records of patients diagnosed with COVID-19 from Jan 20 to Mar 25 from 2 COVID-19 designated centers in Beijing and Anhui province, China. SARS-CoV-2 infection was confirmed by laboratory tests performed by Beijing Center for Disease Control and Prevention (Beijing CDC) and Anhui CDC. The diagnosis of COVID-19 was according to guidelines issued by National Health Commission of China.[6] Only patients with SARS-CoV-2 infection as the only risk factor for liver injury were included in this study. The exclusion criteria included co-infection with any viral hepatitis; presence of other chronic liver diseases (autoimmune hepatitis, primary biliary cholangitis, haemochromatosis and so forth); other viral pathogens co-infection, including influenza A/B, adenovirus, cytomegalovirus and Epstein-Barr virus; receiving long-term medication associated with liver dysfunction; having malignancy. We collected epidemiological, demographic, clinical, routine laboratory, radiological and treatment data for each patient. Severe patients were diagnosed with the criteria that met at least 1 of the following conditions: i) Shortness of breath, respiration rate ≥30 times/min; ii) oxygen saturation (resting state) ≤93%; or iii) PaO2/FiO2 ≤300 mmHg.

In order to identify specific clinical and laboratory features in patients with abnormal liver enzymes, enrolled cases were categorized into 2 groups (with or without aminotransferase abnormality). Sustained alanine aminotransferase (ALT) or aspartate aminotransferase (AST) elevation over the upper limit of normal (40 U/L) ≥7 days during the disease course was defined as liver enzyme abnormality. For each patient, the peak value of ALT or AST among repeated liver function tests during hospitalization was selected for analysis, meanwhile other laboratory parameters obtained simultaneously were recorded. Meanwhile, in this study, liver function abnormality was regarded as abnormal ALT, AST, gamma-glutamyltransferase (GGT), alkaline phosphatase (ALP), albumin, direct bilirubin (DBiL), prothrombin time (PT) or international normalized ratio (INR). Liver synthetic dysfunction was defined as albumin below the lower limit of normal.

After obtaining informed consent, postmortem biopsies of lung and liver tissues from 2 patients who had aminotransferase derangement were used for pathological analysis according to regulations issued by the National Health Commission of China and the Helsinki Declaration.

Chest radiography evaluation

Chest radiographs obtained at the time of peak ALT or AST were retrospectively reviewed and scored in consensus by 3 radiologists who were unaware of the clinical progress of the patients. Scoring was according to the following criteria with 7 stages: 0, bilateral lungs showing clear texture; 1, bilateral lungs showing mild shadows; 2, single small patch shadow; 3, unilateral lung showing multiple patch shadow; 4, bilateral lungs showing multiple patch shadow; 5, unilateral lung showing consolidation; 6, bilateral lung showing consolidation (less than 50%); 7, bilateral lung showing consolidation (more than 50%).

Specimen collection

SARS-CoV-2 diagnostic testing was in accordance with China CDC guidelines. Throat-swab specimens were obtained from patients and maintained in viral-transport medium stored between 2°C and 8°C until ready for shipment to the CDC. Lung and liver tissues were obtained by postmortem biopsies from the 2 patients who died.

Hematoxylin and eosin (H&E) and immunohistochemistry staining

Liver and lung specimens prepared for pathological examination were fixed with 4% neutral formaldehyde, embedded in paraffin wax, and cut into 4 μm sections. Sections were stained with H&E.

Immunohistochemistry was performed to determine the expression of CD68, CD4, CD8, and Ki67 in liver tissues. In detail, the liver biopsies were fixed in 10% formalin for 1.5 h at room temperature, processed for paraffin embedding, and sectioned at a thickness of 4 μm. The sections were incubated with monoclonal antibodies (CD4, CD8, Ki67 and were purchased from Zhongshan Golden Bridge Biotechnology, Beijing, China; CD68 was purchased from Maixin Biotech, Fuzhou, China) overnight at 4°C, and incubated with goat anti-mouse/rabbit secondary antibody (ZSGB-BIO,KIT-5030) for 15 min at 37°C. Subsequently, the sections were developed with diaminobenzidine (DAB) (ZSGB-BIO, ZLI-9018), followed by counterstaining hematoxylin. Immunostained sections were scanned using Leica DFC400 digital camera and Leica Application Suite software (Leica Microsystems).

Transmission electron microscopy (TEM)

TEM was performed to observe ultrastructural changes and SARS-CoV-2 viral particles in liver tissues. In detail, liver biopsy specimens were immediately fixed with 2.5% glutaraldehyde and then postfixed with 1% osmium tetraoxide, dehydrated in a graded series of ethanol concentrations, and embedded in SPIPON812 resin. The ultrathin sections were sectioned with microtome (Leica EM UC6), approximately 70 nm, collected on copper grids and stained by uranyl acetate and lead citrate. Images were taken with a TEM (JEM-1011 120kv).

Terminal deoxynucleotidyl transferase-mediated dUTP nick-end labelling (TUNEL) assay

To detect cell apoptosis, TUNEL assay staining was performed following the manufactures' instructions. Paraffin-embedded sections were prepared and stained with TUNEL reagents after sequential deparaffinization, followed by an apoptosis *in situ* detection kit (Blue Skies, Shanghai, China). DAPI staining was used to visualize nuclei. TUNEL-positive cells labeled with fluorescein isothiocyanate were imaged by NIKON fluorescence microscopy. The frequency of apoptotic cells in liver section was semi-quantified by counting TUNEL-positive cells in 5 microscopic fields per specimen.

Ethical approval

Sample collection and research were in accordance with regulations issued by the National Health Commission of China and the ethical standards formulated in the Helsinki Declaration. Written informed consent was obtained from all patients. The permission for retrospective study was obtained from the institutional review board of The Fifth Medical Center of Chinese PLA General Hospital and The First Affiliated Hospital of Bengbu Medical College.

Statistical analysis

Results for continuous variables were expressed as mean ± SD or median (IQR), as appropriate. Categorical variables were presented as count (percentages). Differences between cases and controls were compared. Continuous variables were compared using Student's *t* test or Mann-Whitney *U* test as appropriate. Categorical variables were compared using Chi-square or Fisher's exact test as appropriate. All statistical tests were 2-sided and statistical significance was set at p <0.05. Analyses were conducted with SAS 9.4 (SAS Institute, Cary, NC).

Results

Characteristics of patients with COVID-19 and abnormal liver aminotransferases

A total of 156 patients with COVID-19 were eligible for this study, including 54 severe cases and 102 non-severe cases, among whom 64 (41.0%) had abnormal liver enzymes, with elevated ALT being the most common abnormality described. Baseline demographic characteristics, clinical features, and treatment regimens were reported in Table 1. The mean age of patients was 51 years old in both groups; 82 (52.6%) patients were male with a similar sex ratio in both groups (59.4% and 47.8%, p = 0.155). In total, 96 (61.5%) cases were reported to either have a history in Hubei (endemic) or have been in close contact with a confirmed COVID-19 patient, and there was no significant difference in the exposure history between the 2 groups. In addition, no significant differences were found with regard to coexisting medical conditions, including diabetes, hypertension, digestive system disease, endocrine system disease, nervous system disease, and chronic respiratory system disease between the 2 groups. The prevalences of initial symptoms were also similar in both groups except that patients with elevated liver enzymes had a greater proportion of cough (73.4% *vs.* 56.5, p = 0.031). Importantly, we found that liver aminotransferase abnormality was associated with disease severity (p = 0.007) and higher radiology scores (p = 0.007). Specifically, 30 of 54 (55.6%) severe cases and 24 of 102 (23.5%) non-severe cases presented with elevated liver enzymes. Nine severe patients, including 5with acute respiratory distress syndrome (ARDS), 2 with sepsis, 1 with acute kidney injury and 1 with uremia were admitted to the intensive care unit (ICU), among whom 7 (77.8%) cases presented with liver enzyme abnormality. The medication details of patients admitted to the ICU, as well as their liver function tests, were summarized in Table S1. In our study, all patients received antiviral therapy with PEG-Interferon α2b, lopinavir/ritonavir or both. Half of the patients were given antibiotic treatment and 26.3% patients were given systematic corticosteroids. Additionally, 26.9% patients were given immunoglobulin therapy. The treatment regimens were not significantly different between abnormal and normal aminotransferase groups. Of the 156 patients, the overall mortality rate was 2.6% (n = 4). Mortality occurred in 3 (4.7%) patients with liver enzyme abnormality (ARDS in 2 and septic shock in 1) and 1 (1.1%) patient with normal liver enzymes (septic shock). The median duration of hospitalization was 19 days and 15 days (p = 0.127), respectively, in patients with abnormal and normal liver enzymes.

A comparison of laboratory characteristics between patients with or without liver enzyme abnormality was summarized in

Table 1. Demographic and clinical characteristics.*

Characteristics	Patients with abnormal aminotransferases n = 64	Patients with normal aminotransferases n = 92	*p* value
Age (year)	51.1 ± 17.4	51.2 ± 15.2	0.962
Sex			
Male	38 (59.4)	44 (47.8)	0.155
Female	26 (40.6)	48 (52.2)	
Exposure			
Hubei province exposure	20 (31.3)	25 (27.2)	0.580
Close contact with COVID-19 patient	21 (32.8)	41 (44.6)	0.140
All of the above	5 (7.8)	6 (6.5)	1.000
No exposure	28 (43.8)	32 (34.8)	0.258
Coexisting medical conditions			
Diabetes	9 (14.1)	8 (8.7)	0.290
Hypertension	20 (31.3)	22 (23.9)	0.310
Digestive system disease	1 (1.6)	5 (5.4)	0.402
Endocrine system disease	1 (1.6)	2 (2.2)	1.000
Nervous system disease	2 (3.1)	2 (2.2)	1.000
Chronic respiratory system disease	4 (6.3)	4 (4.4)	0.717
Other underlying disease	–	–	–
Signs and symptoms			
Fever	60 (93.8)	83 (90.2)	0.432
Cough	47 (73.4)	52 (56.5)	0.031
Myalgia or fatigue	18 (28.1)	34 (37.0)	0.250
Sputum production	22 (34.4)	26 (28.3)	0.416
Headache	10 (15.6)	14 (15.2)	0.945
Hemoptysis	1 (1.6)	2 (2.2)	1.000
Diarrhea	6 (9.4)	12 (13.0)	0.481
Dyspnea	12 (18.8)	22 (23.9)	0.442
Sore throat	7 (10.9)	17 (18.5)	0.199
Rhinorrhea	2 (3.1)	1 (1.1)	0.568
Chest pain	3 (4.7)	2 (2.2)	0.401
Nausea and vomiting	1 (1.6)	4 (4.4)	0.649
Severe patients	30 (46.9)	24 (26.1)	0.007
Radiology scores#			0.007
0–3	33.3%	66.7%	
4–7	66.7%	33.3%	
Treatment			
PEG-interferon α2b	59 (92.2)	85 (92.4)	1.000
Lopinavir/ritonavir	38 (59.4)	57 (62.0)	0.745
Antibiotic treatment	33 (51.6)	40 (43.5)	0.320
Use of corticosteroid	20 (31.3)	21 (22.8)	0.240
Intravenous immunoglobulin therapy	19 (29.7)	23 (25.0)	0.516
Mortality	3 (4.7)	1 (1.1)	0.306
Hospitalization days	19 (14–24)	15 (12–23)	0.127

*Normally distributed continuous variables were expressed in mean ± SD, whereas other continuous variables were expressed in median (IQR). Categorical variables were presented as counts (percentage). Qualitative and quantitative differences between two groups were analyzed by Chi-square test or Fisher exact test for categorical parameters and Student's *t* test or Mann-Whitney *U* test for continuous parameters as appropriate. Levels of significance: p <0.05.
#Data of chest scores were available in 27 patients with abnormal aminotransferases and 42 patients with normal aminotransferases, respectively.

Table 2. Laboratory characteristics.*

Variables	Patients with abnormal aminotransferases n = 64	Patients with normal aminotransferases n = 92	*p* value
Arterial blood gas			
PO_2 80–100 (mmHg)	83.5 (79.5–92.0)	92.0 (80.0–126.0)	0.341
TCO_2 23–27 (mmol/L)	24.9 (23.9–28.6)	27.0 (26.2–28.4)	0.325
CL 93–100 (mmol/L)	104 (99–106)	103 (100–105)	0.617
Anion gap 23–65 (mmol/L)	12.0 (9.1–15.8)	12.6 (11.3–16.9)	0.443
SaO_2 95–100 (%)	96 (96–97)	97 (96–99)	0.344
A-aDO_2 10–15 (mmHg)	202.0 (30.5–331.2)	27.6 (15.2–37.7)	0.022
O_2Cont 7.5–23 (vol%)	17.3 (15.1–18.8)	18.8 (17.4–20.4)	0.088
P50 25–29 (mmHg)	25.7 (25.2–26.9)	26.7 (25.3–28.8)	0.323
Lactic acid 0.6–2.2 (mmol/L)	2.1 (1.8–2.4)	2.0 (1.5–2.9)	0.559
Biochemical tests			
Liver enzymes			
ALT 5–40 (U/L)	50.0 (40.0–70.0)	19.0 (14.6–28.5)	<0.001
AST 5–40 (U/L)	45.5 (38.0–60.0)	24.0 (19.7–29.0)	<0.001
AST/ALT	0.89 (0.60–1.36)	0.96 (0.72–1.38)	0.498
ALP 40–150 (U/L)	61 (49–76)	63 (48–76)	0.842
GGT 11–50 (U/L)	45 (28–78)	22 (15–40)	<0.001
Ratio of abnormality	45%	22%	0.002
Liver function			
Total protein 60–83(g/L)	68 (63–73)	69 (64–73)	0.773
Albumin 35–55(g/L)	37 (33–41)	39 (36–41)	0.067
Ratio of abnormality	38.1%	20.7%	0.017
Globumin 20–40(g/L)	32 (28–35)	30 (27–33)	0.097
TBiL 3.4–20.5 (μmol/L)	10.5 (8.2–15.4)	9.5 (7.1–15.4)	0.286
Ratio of abnormality	14%	13%	0.855
DBiL 0–6.8 (μmol/L)	3.6 (2.4–6.4)	3.1 (1.8–5.3)	0.141
Ratio of abnormality	23%	12%	0.058
TBA 0–10 (μmol/L)	3.0 (1.9–5.9)	2.6 (1.4–3.8)	0.185
Ferritin 30–400 (ng/ml)	632.7 (339.1–1,128.0)	300.0 (95.3–429.8)	<0.001
Ratio of abnormality	68%	40%	0.027
Other biochemical tests			
Lactate dehydrogenase 109–245 (U/L)	279 (218–399)	218 (187–271)	<0.001
Adenosine deaminase 0–20 (U/L)	17.1 (12.0–24.9)	13.7 (11.0–20.2)	0.059
Cholinesterase 5000–12000 (U/L)	7,221 (5522–8,016)	7,151 (5987–8,211)	0.405
Leucine aminopeptidase 39–80 (U/L)	61 (50–68)	49 (42–56)	0.007
Blood urea nitrogen 2.9–8.2 (mmol/L)	4.7 (3.8–5.6)	3.7 (3.2–4.5)	0.004
Creatine kinase 26–140 (U/L)	81.5 (42.0–232.5)	54.0 (36.0–88.0)	0.004
Creatinine 62–115 (μmol/L)	66.5 (50.7–79.5)	67.5 (55.6–80.5)	0.781
Uric acid 208–428 (μmol/L)	231 (174–316)	234 (175–301)	0.654
Glucose 3.9–6.1 (mmol/L)	6.0 (5.2–8.0)	5.3 (4.8–6.3)	0.005
Total cholesterol 2.8–5.2 (mmol/L)	3.8 (3.2–4.4)	3.9 (3.5–4.5)	0.443
Triglyceride 0.56–1.7 (mmol/L)	1.15 (0.93–1.74)	1.20 (0.92–1.69)	0.652
HDL-c 1.29–1.55 (mmol/L)	0.96 (0.83–1.19)	1.00 (0.83–1.23)	0.447
LDL-c 2.1–3.1 (mmol/L)	2.37 (2.01–3.01)	2.40 (1.90–2.96)	0.903
Apolipoprotein A1 1.05–2.05 (g/L)	0.91 (0.74–1.03)	1.00 (0.79–1.14)	0.049
Apolipoprotein B 0.55–1.30 (g/L)	0.85 (0.66–1.07)	0.77 (0.64–0.95)	0.238
Lipoprotein (a) 0–300 (mg/L)	184 (62–303)	180 (101–352)	0.668
Coagulation function			
INR 0.8–1.2	1.05 (1.00–1.10)	1.05 (0.99–1.10)	0.329
Prothrombin time 10.2–14.3 (sec)	12.1 (11.5–12.6)	11.8 (11.3–12.5)	0.223
D-dimer <0.55 (mg/L)	0.53 (0.24–1.10)	0.37 (0.22–0.68)	0.032
Routine blood tests			
WBC 3.97–9.15 (10^9/L)	5.7 (4.5–8.2)	5.2 (3.9–6.6)	0.022
NEUT 2–7 (10^9/L)	3.90 (2.61–5.72)	3.10 (2.19–4.01)	0.010
LYMPH 0.8–4.0 (10^9/L)	1.20 (0.75–1.86)	1.40 (1.15–1.81)	0.090
Absolute monocyte 0.12–1.0 (10^9/L)	0.46 (0.27–0.59)	0.38 (0.28–0.55)	0.194
Absolute eosinophil 0.02–0.5 (10^9/L)	0.02 (0.01–0.11)	0.07 (0.01–0.12)	0.183
Absolute basophilic 0–1 (10^9/L)	0.02 (0.01–0.03)	0.01 (0.01–0.03)	0.278
RBC 4.09–5.74 (10^{12}/L)	4.27 (3.85–4.71)	4.34 (3.86–4.70)	0.579
ESR 0–15 (mm/60min)	32.9 (17.0–59.0)	23.8 (10.0–51.5)	0.326
Hemoglobin 131–172 (g/L)	129 (118–144)	131 (120–141)	0.655
PCV 38–50.8 (%)	39.0 (35.7–42.6)	39.0 (35.3–42.5)	0.742
MCV 83.9–99.1 (fL)	91.6 (87.1–95.5)	91.4 (88.0–94.7)	0.789
MCHC 27.8–33.8 (pg)	30.4 (29.0–31.7)	30.4 (29.2–31.5)	0.988
RDW 0–15 (%)	13.2 (12.5–44.3)	13.1 (12.5–40.8)	0.230
PLT 85–303 (10^9/L)	186 (139–250)	199 (155–252)	0.319

(*continued on next page*)

Table 2. (*continued*)

Variables	Patients with abnormal aminotransferases n = 64	Patients with normal aminotransferases n = 92	*p* value
PCT 0.06–0.40 (%)	0.21 (0.16–0.25)	0.22 (0.17–0.28)	0.220
MPV 7.54–11.24 (fL)	9.5 (8.4–10.6)	9.7 (8.8–10.7)	0.611
PDW 9.0–18.0 (%)	14.0 (11.8–15.9)	12.5 (11.1–15.8)	0.099
P-LCR 13–43 (%)	26.5 (23.2–33.4)	26.1 (22.3–31.4)	0.490
Lymphocytes			
T LYMPH 690–2540 (/μl)	455 (303–1,358)	891 (631–1,045)	0.171
CD4 LYMPH 410–1590 (/μl)	240 (106–606)	470 (344–616)	0.024
CD8 LYMPH 190–1140 (/μl)	236 (116–531)	367 (228–509)	0.241
B LYMPH 90–660 (/μl)	86 (51–174)	150 (107–196)	0.025
NK LYMPH 90–590 (/μl)	124 (51–186)	161 (122–221)	0.051
CD4/CD8 0.68–2.47	1.20 (0.79–1.67)	1.20 (0.95–1.63)	0.537
Infection related biomarkers			
C-reactive protein 0.068–8.2 (mg/L)	19.5 (3.2–57.6)	9.8 (2.4–35.2)	0.156
Interleukin-6 (pg/ml)	4.7 (1.9–13.7)	7.1 (3.7–16.4)	0.255
Procalcitonin 0–0.5 (ng/ml)	0.04 (0.02–0.09)	0.04 (0.02–0.06)	0.290

A-aDO_2, alveolar-arterial oxygen partial pressure difference; ALP, alkaline phosphatase; ALT, alanine aminotransferase; AST, aspartate aminotransferase; DBiL, direct bilirubin; ESR, erythrocyte sedimentation rate; GGT, gamma-glutamyltransferase; HDL-c, high density lipoprotein cholesterol; INR, international normalized ratio; LDL-c, low density lipoprotein cholesterol; LYMPH, absolute lymphocyte value; MCHC, mean corpuscular hemoglobin concentration; MCV, mean corpuscular volume; MPV, mean platelet volume; NEUT, absolute neutrophil count; NK, natural killer cell; O2Cont, oxygen content of blood; P50, oxygen half-saturation pressure of hemoglobin; PCT, platelet cubic measure distributing; PCV, packed cell volume; PDW, platelet distribution width; PLT, platelet count; *P*-LCR, platelet-large cell ratio; PO_2, oxygen partial pressure; PT, Prothrombin time; RBC, red blood cell; RDW, red cell distribution width; SaO, oxygen saturation; TBA, total bile acid; TBiL, total bilirubin; TCO2, total carbon dioxide; WBC, white blood cells.

*Normally distributed continuous variables were expressed in mean ± SD, whereas other continuous variables were expressed in median (IQR). Categorical variables were presented as percentage. Qualitative and quantitative differences between two groups were analyzed by Chi-square test or Fisher exact test for categorical parameters as appropriate and Mann-Whitney *U* test for continuous parameters. Levels of significance: p <0.05.

Table 2. In terms of arterial blood gas tests, the median alveolar-arterial oxygen tension difference (A-aDO_2) was dramatically higher in patients with abnormal liver enzymes than those with normal liver enzymes (202.0 *vs.* 27.6, p = 0.022). In the abnormal and normal aminotransferase groups, the median levels of ALT and AST were 50 U/L *vs.* 19 U/L (p <0.001) and 45.5 U/L *vs.* 24 U/L (p <0.001), respectively. Compared to patients with normal aminotransferases, patients who had elevated aminotransferases presented higher levels of GGT but similar levels of ALP. In addition to liver enzymes, liver dysfunction as indicated by other common parameters, including lower albumin, higher DBiL and ferritin tended to be more frequent in patients with elevated liver enzymes than those with normal liver enzymes (p = 0.017, p = 0.058, p = 0.027), while the levels of total protein, globulin, and total bile acid were normal and did not vary significantly between the 2 groups. Patients with abnormal liver enzymes had elevated levels of lactate dehydrogenase, leucine aminopeptidase, urea nitrogen, creatine kinase, glucose and D-dimer. No significant differences in INR and PT were found between the two groups. The blood routine tests were comparable between the 2 groups except for higher WBC and absolute neutrophil counts in patients with elevated aminotransferases (p = 0.022 and p = 0.010), despite the median values being in normal ranges. Blood levels of total lymphocytes (455 *vs.* 891 /μl, p = 0.171), CD4+ lymphocytes (240 *vs.* 470 /μl, p = 0.024) and B lymphocytes (86 *vs.* 150 /μl, p = 0.025) were all markedly decreased in the abnormal aminotransferase group, although there was no statistically significant difference for total lymphocytes. No significant differences in serum C-reactive protein, interleukin-6 (IL-6) or procalcitonin were observed between the 2 groups.

Liver histological and immunohistochemical findings

Case 1

Case 1 was a 50-year-old man presenting with mild initial symptoms one week prior to being admitted to hospital (day 8). He had a travel history to Wuhan before onset of symptoms. Interferon alfa-2b and lopinavir plus ritonavir were administered as antiviral therapy, and moxifloxacin was used to prevent secondary infection. However, the patient's symptoms did not improve, and his hypoxemia and shortness of breath got worse. On day 12, a chest x-ray showed progressive infiltrate and diffuse gridding shadow in the bilateral lungs. His pulmonary function rapidly deteriorated and he died of ARDS on day 14. He had elevated aminotransferases during the whole disease course with peak ALT and AST of 70 U/L and 111 U/L, respectively.

Histologic examination of lung tissue revealed diffuse alveolar damage (DAD), prominent desquamation of pneumocytes and hyaline membrane formation, indicating a severe acute lung injury (Fig. 1A). Liver biopsy showed substantial cluster or scattered apoptotic hepatocytes characterized by condensed nuclear or formed apoptotic bodies (Fig. 1B). Prominent binuclear or occasional multinuclear syncytial hepatocytes were identified. No obvious viral inclusions were identified. Moderate microvesicular and mild macrovesicular steatosis were observed. Other pathologic manifestations included mild to moderate focal lobular inflammation with infiltration of predominant lymphocytes and few neutrophils. Mild inflammation in the portal tracts with lymphocytic infiltrate was occasionally noted. There was no eosinophil cell infiltration, cholestasis, granuloma, fibrin deposition, centrilobular necrosis, or interface hepatitis.

Immunohistochemistry revealed increased CD68+ cells mainly distributed in hepatic sinusoids (50–60 positive cell counts per 200× power field), suggesting Kupffer cell activation (Fig. 1C). CD4+ cells were infrequently presented (3–5 positive cell counts per 400× power field) (Fig. 1D). A few CD8+ cells were scattered in liver lobule and portal areas (5–15 positive cell counts per 400× power field) (Fig. 1E). There was some Ki-67 positive staining in hepatocytes and infiltrated mononuclear cells (8–10 positive cell counts per 400× power field) (Fig. 1F).

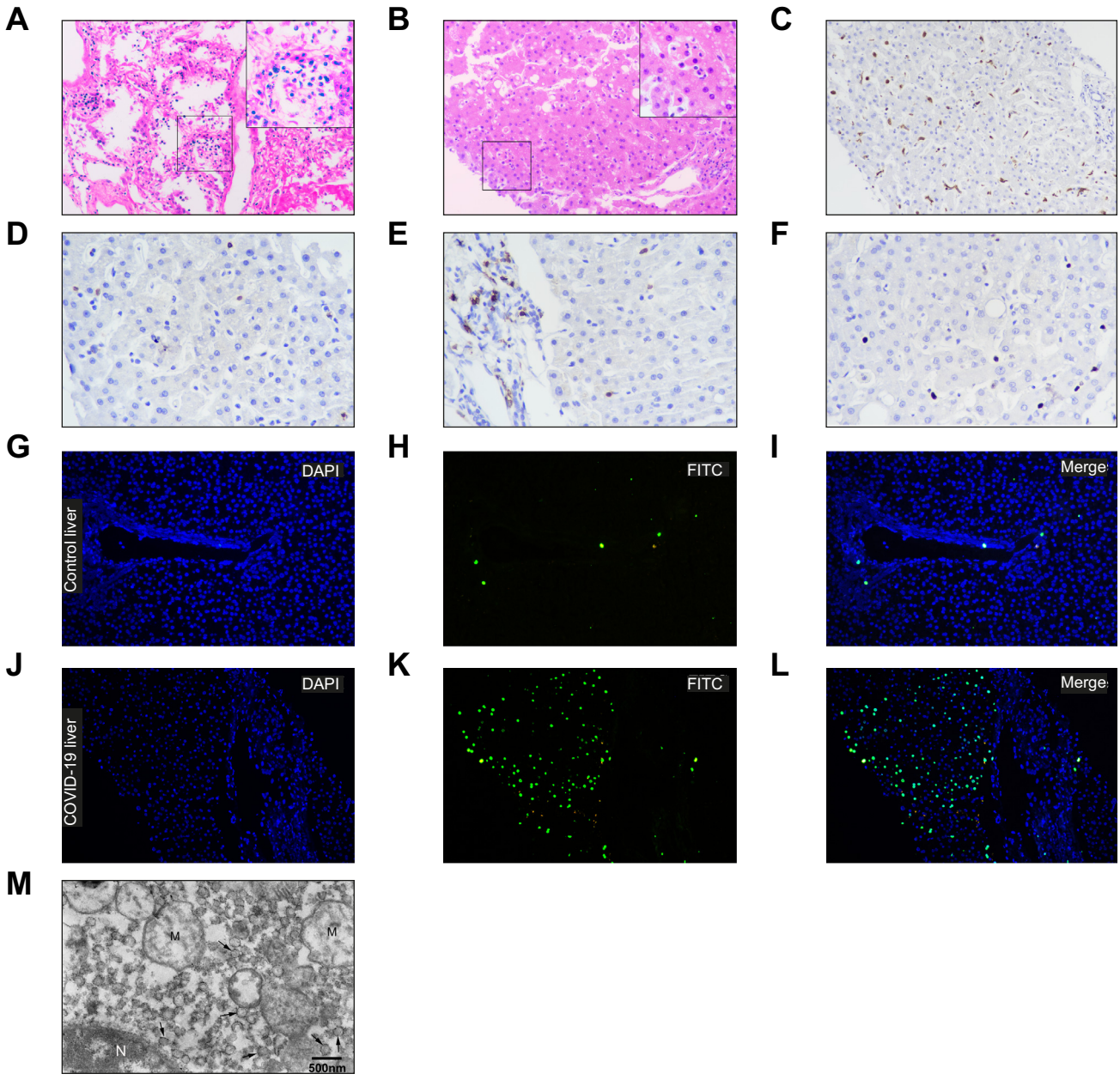

Fig. 1. Postmortem biopsy specimens from case 1. (A) Lung tissue showing diffuse alveolar damage, desquamation and hyaline membrane, and multinucleated syncytial pneumocytes, as well as interstitial mononuclear infiltrates (H&E staining, original magnification ×200, up-right region original magnification ×400). (B) Liver tissue showing substantial apoptotic hepatocytes, prominent binuclear hepatocytes, and mild to moderate steatosis. (H&E staining, original magnification ×200, up-right region original magnification ×400). (C) Immunohistochemistry of liver tissue revealing activated CD68+ cells (original magnification ×200), (D) scattered CD4+ cells and (E) CD8+ cells in lobular and portal areas (original magnification ×400). (F) Nuclear proliferative antigen Ki-67 was positive in a few mononuclear cells and hepatocytes (original magnification ×400). TUNEL staining (green) showing apoptotic cells in control liver tissue (G–I) and in COVID-19 liver tissue (J–L). DAPI (blue) was applied to visualize nuclei. (M) Ultrastructural examination identifying amounts of typical coronavirus particles (arrow) with size of 60–120 nm in cytoplasm of hepatocytes. Ultrastructural impairment manifesting conspicuous mitochondria (marked as M) swelling and glycogen granule decrease (original magnification ×15,000). COVID-19, coronavirus disease 2019.

TUNEL-positive cells with green florescence in nuclei indicated apoptotic cells. Peri-hemangioma liver tissue from one hepatic hemangioma case was used as a control (Fig. 1G–I). Apoptotic hepatocytes were abundant in the liver of the patient with COVID-19 (80–120 positive cell counts per 200× power field) compared to the control liver (5–8 positive cell counts per 200× power field) (Fig. 1G–L).

TEM examination identified the typical coronavirus particles in the cytoplasm of hepatocytes, and most viral particles existed without membrane-bound vesicles (Fig. 1M). The virions were round, mildly pleomorphic, and showed surface thickening indicative of the corona peplomer structure, with size ranges between 60–120 nm. Intriguingly, SARS-CoV-2-infected hepatocytes exhibited marked swelling mitochondria with obscure

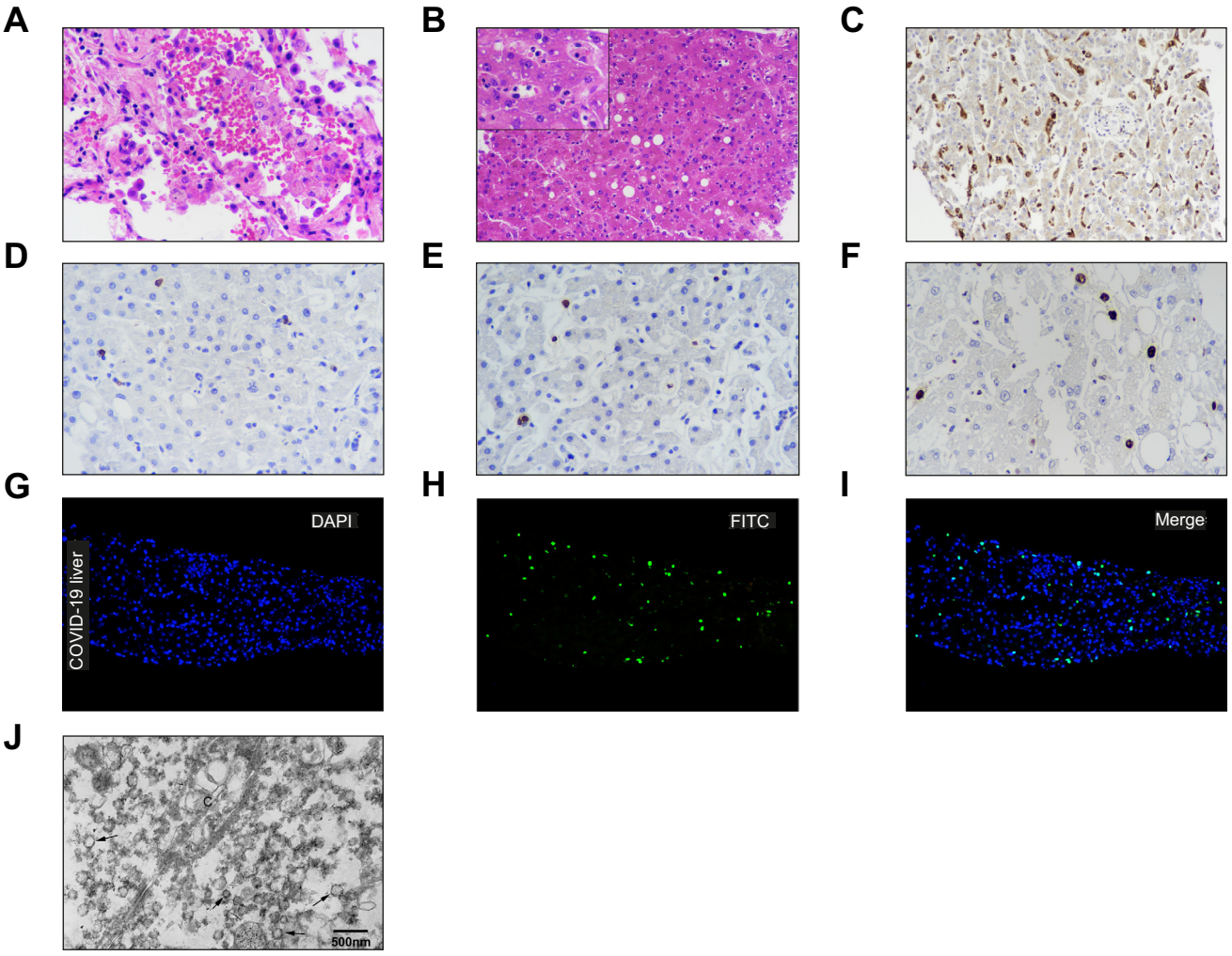

Fig. 2. Postmortem biopsy specimens from case 2. (A) Lung tissue showing late phase diffuse alveolar damage, with cellular and fibrinous exudation, hemorrhage, and foamy cells in alveolar spaces (H&E staining, original magnification ×400). (B) Liver tissue revealing abundant apoptotic hepatocytes, plenty of binuclear cells, and mild to moderate micro- and macrovesicular steatosis (H&E staining, original magnification ×200). (C) Immunohistochemistry for liver tissue revealing numerous activated CD68+ Kupffer cells (original magnification ×200), (D) scattered CD4+ and (E) CD8+ cells in lobules (original magnification ×400). (F) A few Ki67 positive proliferative hepatocytes and Kupffer cells (original magnification ×400). (G–I) TUNEL assay displaying apoptotic hepatocytes (green). (J) Electron microscopy showing numerous coronavirus particles (arrow) in cytoplasm of hepatocytes. The pattern of cell damage including decreased glycogen granules and canalicular (marked as C) impairment with shedding of microvilli (original magnification ×12,000).

cristae or high electronic density materials, strongly indicating that SARS-CoV-2 directly caused cytopathy. Moderate density fats were observed and glycogen granules were apparently decreased in hepatocytes.

Case 2

Case 2 was a 79-year old female admitted to hospital with repeated fever, fatigue, dizziness, myalgia, and cough. She reported a close contact with her daughter who had SARS-CoV-2 infection. Despite receiving antiviral and antibacterial medications, her situation worsened and she developed respiratory failure and hemorrhagic shock on day 11 and day 18, respectively. SARS-CoV-2 RNA test was still positive on day 24. On day 26, she suddenly developed chills and hyperpyrexia. Chest X-ray images showed a rapid deterioration of pneumonia. Meanwhile, *Klebsiella pneumoniae* was identified in both blood and sputum samples. This patient died of septic shock on day 28. Her liver enzymes increased gradually during the last few days with peak ALT and AST of 76 and 236 U/L.

The lung pathological feature indicated late phase DAD and loose interstitial fibrosis with admixed areas of fibrinous exudation and edema in alveolar space (Fig. 2A). Liver biopsy showed quite similar histology to the case 1 with conspicuous multi-focal or scanty apoptotic bodies (Fig. 2B). There were plenty of binuclear or occasional multinuclear cells with apparent nucleoli and congregated chromatin. Moderate microvesicular and mild macrovesicular steatosis were also observed. The portal inflammation was very mild. No centrilobular necrosis, ductular/canalicular cholestasis, vasculitis, interface hepatitis, or hemophagocytosis were identified.

Immunohistologically, numerous CD68+ cells with larger size were seen predominantly in sinusoids (150–200 counts per 200× power field) (Fig. 2C). Scattered CD4+ cells and CD8+ cells appeared in lobules (Fig. 2D–E). There was some Ki67 positive

staining in hepatocytes and Kupffer cells (5–10 positive cell counts per 400× power field) (Fig. 2F).

TUNEL assay displayed plenty of apoptotic hepatocytes in this patient (60–120 positive cell counts per 200× power field), like case 1 (Fig. 2G–I)

TEM showed numerous coronavirus particles with size ranges between 70–120 nm in the cytoplasm without membrane-bound vesicles in hepatocytes (Fig. 2J). The majority of viral particles were intact, but a few fragmented virions were also visible. High electronic density lipid droplets were noted. The pattern of cell damage included glycogen granule decrease in hepatocytes and canalicular impairment with shedding of microvilli, suggesting a cytopathic lesion caused by SARS-CoV-2 infection.

Discussion

Coronaviruses have a broad host range and cause a wide variety of respiratory, gastrointestinal, and systemic diseases in animals and humans. Liver enzyme abnormalities developed in as many as 50% of SARS-CoV-2-infected patients reported by various studies. In our study, 41.0% of patients with COVID-19 presented with liver enzyme abnormality, with a prevalence of 23.5% even in the context of mild cases, confirming liver impairment is common in patients with COVID-19. The liver enzyme abnormality was associated with disease severity, as well as a series of laboratory tests, including higher A-aDO_2, higher FER, lower albumin, and decreased circulating CD4+ T cells and B lymphocytes. Importantly, we provided the first evidence of SARS-CoV-2 infection directly causing cytopathy of hepatocytes and impairing liver function in patients with COVID-19, although other factors such as drug toxicity or complication-related insults to the liver cannot be excluded.

SARS-CoV was also reported to cause liver impairment.[7,8] However, the evidence of visible coronavirus particles under TEM examination in liver tissue was absent.[9,10] In this study, abundant SARS-CoV-2 viral particles were observed in the cytoplasm of hepatocytes in two COVID-19 cases. The majority of viral particles were noted to harbor a complete envelope with corona-like spikes, indicating SARS-CoV-2 is not only able to enter, but also replicate in hepatocytes. Strikingly, ultrastructural features of conspicuous mitochondria swelling, endoplasmic reticulum dilatation, and impaired cell membrane demonstrated the cytopathy of SARS-CoV-2 in hepatocytes. Moreover, massive hepatic apoptosis and binuclear or a few multinuclear hepatocytes, which were syncytial, rather than proliferative identified by Ki67 immunohistochemistry, were the predominant histological features of viral infection. Meanwhile, immunohistochemistry results showed scarce CD4+ cells and CD8+ cells in liver tissues, suggesting immunopathologic insult might not be favored in liver damage. Taken together, histological and ultrastructural evidence indicated that SARS-CoV-2 dissemination in the liver potentially contributed to abnormal liver aminotransferases.

Angiotensin-converting enzyme 2 (ACE2) is known as cell entry receptor of both SARS-CoV and SARS-CoV-2.[2,11] SARS-CoV-2 is perceived to be less likely to cause liver infection due to lower ACE2 expression in hepatocytes. However, we found abundant SARS-CoV-2 viral particles in hepatocytes. Usually, the receptor distribution is considered to be concordant with that of infected organs. Nevertheless, there exist notable discordances of ACE2 expression in SARS-CoV targeted multiorgans,[12,13] such as virus replication in colonic epithelium, which has no ACE2, and no virus infection in endothelial cells, which have ACE2.[14] Evidently, these discrepancies suggested the localization of ACE2 does not fully explain the liver tropism of SARS-CoV-2. We speculate that alternative extra-ACE2 receptors or co-receptors might exist. Another possibility is that the expression of ACE2 in hepatocytes may be upregulated upon sensing virus entry. However, we have no data on the expression of ACE2 in SARS-CoV-2-infected liver and further study is required to address this hypothesis.

One of the striking observations in our study was that the A-aDO_2 was dramatically higher in patients with liver aminotransferase abnormality, implying that liver damage may be linked to poor pulmonary function in patients with COVID-19. Mechanistically, proinflammatory cytokines were reported to increase significantly in severe COVID-19 cases.[4,15] This event often provokes systemic ischemia and hypoxia, which is blamed for inadequate pulmonary ventilation, manifesting as an elevation of A-aDO_2. Thus, patients with severe COVID-19 may be predisposed to developing hypoxic-ischemic liver injury. The hallmark of ischemic liver injury is centrilobular necrosis, usually identified by acute and marked increases in serum aminotransferases.[16,17] The 2 biopsied cases in the current study did not present the pathological feature of ischemic liver and their serum aminotransferases were increased moderately, implicating the liver impairment in these 2 cases might be independent of pulmonary dysfunction to an extent. Additionally, the involvement of other COVID-19-related complications in liver enzyme abnormality cannot be ruled out. There were only 2 septic patients in our study, 1 with elevated liver enzymes (case 2) and the other with normal liver enzymes, suggesting that sepsis is unlikely to contribute to the high incidence of liver enzyme abnormality in the current cohort. Additionally, the pathological examination in case 2 showed no septic histological features of centrilobular necrosis, canalicular/ductular cholestasis, non-bacterial cholangitis, suggesting that septic insult is unlikely to be the main cause of liver impairment in this case. Nevertheless, due to the limited number of septic patients in our cohort, we could not provide convincing data on the frequency of liver function abnormality in septic patients.

Drug-induced liver injury (DILI) might be an alternative cause of liver damage. According to our results, no significant differences in terms of antiviral and antibiotic medications were found between normal and abnormal liver enzyme groups. Moreover, as hepatotoxicity usually occurs after long-term antiviral therapy, the clinical courses of our patients did not favor antiviral DILI. Indeed, hepatotoxicity may occur in the first few weeks after antibiotic therapy and are typically related to remarkable elevation of liver enzymes, sometimes in conjunction with allergic reactions such as rash. However, our patients had no such obvious adverse reactions, and the median ALT level was 50 (40.0–70.0) U/L in this cohort. Histologically, although both SARS-CoV-2 infection and drugs might result in liver steatosis,[18–20] the pathological features of no obvious eosinophil infiltration, cholestasis, fibrin deposition, granuloma, massive central necrosis, or interface hepatitis in the 2 biopsied cases were not suggestive of DILI. Nevertheless, we could not exclude DILI as a participating cause since only 2 cases were biopsied.

Several other laboratory variables were shown to associate with aminotransferase abnormalities in COVID-19. The median GGT values in both groups of abnormal and normal aminotransferases were in normal range and no significant differences in levels of DBiL, total bilirubin, or ALP were observed between the 2

groups, suggesting that bile ducts were unlikely the SARS-CoV-2 target sites. Notably, patients with elevated liver enzymes were more likely to have lower serum albumin, suggesting an association of liver synthetic dysfunction and liver enzyme abnormality in patients with COVID-19. Serum ferritin levels were higher in patients with elevated aminotransferases. Physiologically, one-third of ferritin is stored in the liver and circulating ferritin can normally be cleared by liver cells. Therefore, patients with damaged livers may fail to get rid of circulating ferritin, leading to an accumulation of ferritin in serum. Immune disruption, characterized by lymphopenia, decreased levels of CD4+ T cells and B lymphocytes, was more profound in the group with abnormal aminotransferases. However, the serum IL-6 was not higher, but even lower in patients with abnormal aminotransferases. Besides, both lymphopenia and elevated liver enzymes were linked to the severity of COVID-19. We thereafter assumed that immune dysfunction and liver impairment were coincident events, rather than having a cause-effect relationship.

There were limitations in our study. We could only conduct ultrastructural and pathological analysis in 2 biopsies, which is insufficient to represent the entire cohort. Moreover, the cohort was limited to 2 centers. Therefore, large- and multi-cohort studies that contain more cases available for biopsy or autopsy are justified to comprehensively understand liver impairment in COVID-19 patients. However, we believe that our remarkable findings offered crucial clue to liver enzyme abnormality in COVID-19 patients.

In this study, we identified the clinical and laboratory characteristics of COVID-19 patients with abnormal liver aminotransferases and firstly reported SARS-CoV-2 is able to infect liver and cause liver impairment of conspicuous cytopathy. In this perspective, a surveillance of viral clearance in liver and long-term outcome of COVID-19 is required. Additional researches on how and to what extent that SARS-COV-2 infection involved in liver enzyme abnormality in distinct COVID-19 population are required.

Abbreviations

A-aDO_2, alveolar-arterial oxygen partial pressure difference; ACE2, angiotensin-converting enzyme 2; ALP, alkaline phosphatase; ALT, alanine aminotransferase; ARDS, acute respiratory distress syndrome; AST, aspartate aminotransferase; COVID-19, coronavirus disease 2019; DAD, diffuse alveolar damage; DILI, drug-induced liver injury; DBil, direct bilirubin; GGT, gamma-glutamyltransferase; H&E, hematoxylin and eosin; ICU, intensive care unit; IL-6, interleukin-6; INR, international normalized ratio; PT, prothrombin time; SARS-CoV-2, severe acute respiratory syndrome coronavirus 2; TBA, total bile acid; TEM, transmission electron microscopy; TUNEL, terminal deoxynucleotidyl transferase-mediated dUTP nick-end labelling; WBC, white blood cells.

Financial support

The authors received no financial support to produce this manuscript.

Conflict of interest

The authors declare no conflicts of interest that pertain to this work.

Please refer to the accompanying ICMJE disclosure forms for further details.

Authors' contributions

JZ contributed to study concept and design, clinical and pathological analysis, study supervision and critical revision of the manuscript; YW contributed to study design, analysis and interpretation of data, literature search and writing of the manuscript; SL contributed to specimen collection and pathological and immunohischemical analysis; HL contributed to data analysis, making tables, and literature search; FL and JM contributed to clinical data analysis; WL, YC, LJ, XLi, XL and SZ contributed to clinical data collection; JL and JK contributed to electron microscope imaging and analysis; PX, LZ, JY, LL, YL contributed to pathological and immunohischemical experiments; LZ contributed to making figures; RN contributed to literature search; CZ and JJ contributed to clinical data collection and analysis; FL contributed to data analysis.

Supplementary data

Supplementary data to this article can be found online at https://doi.org/10.1016/j.jhep.2020.05.002.

References

Author names in bold designate shared co-first authorship

[1] **Zhu N, Zhang D, Wang W, Li X, Yang B,** Song J, et al. A novel coronavirus from patients with pneumonia in China, 2019. N Engl J Med 2020;382:727–733.
[2] **Zhou P, Yang XL, Wang XG,** Hu B, Zhang L, Zhang W, et al. A pneumonia outbreak associated with a new coronavirus of probable bat origin. Nature 2020;579:270–273.
[3] **Xu XW, Wu XX,** Jiang XG, Xu KJ, Ying LJ, Ma CL, et al. Clinical findings in a group of patients infected with the 2019 novel coronavirus (SARS-Cov-2) outside of Wuhan, China: retrospective case series. BMJ 2020;368:m606.
[4] **Huang C, Wang Y, Li X, Ren L, Zhao J,** Hu Y, et al. Clinical features of patients infected with 2019 novel coronavirus in Wuhan, China. Lancet 2020;395:497–506.
[5] **Chen N, Zhou M, Dong X, Qu J,** Gong F, Han Y, et al. Epidemiological and clinical characteristics of 99 cases of 2019 novel coronavirus pneumonia in Wuhan, China: a descriptive study. Lancet 2020;395:507–513.
[6] The New Coronavirus Pneumonia Prevention and Control Program. National Health Commission of China. 5th ed. China: National Health Commission of China; 2020.
[7] Lee N, Hui D, Wu A, Chan P, Cameron P, Joynt GM, et al. A major outbreak of severe acute respiratory syndrome in Hong Kong. N Engl J Med 2003;348:1986–1994.
[8] Tsang KW, Ho PL, Ooi GC, Yee WK, Wang T, Chan-Yeung M, et al. A cluster of cases of severe acute respiratory syndrome in Hong Kong. N Engl J Med 2003;348:1977–1985.
[9] Chau TN, Lee KC, Yao H, Tsang TY, Chow TC, Yeung YC, et al. SARS-associated viral hepatitis caused by a novel coronavirus: report of three cases. Hepatology 2004;39:302–310.
[10] Poutanen SM, Low DE, Henry B, Finkelstein S, Rose D, Green K, et al. Identification of severe acute respiratory syndrome in Canada. N Engl J Med 2003;348:1995–2005.
[11] **Li W, Moore MJ,** Vasilieva N, Sui J, Wong SK, Berne MA, et al. Angiotensin-converting enzyme 2 is a functional receptor for the SARS coronavirus. Nature 2003;426:450–454.
[12] Hamming I, Timens W, Bulthuis ML, Lely AT, Navis G, van Goor H. Tissue distribution of ACE2 protein, the functional receptor for SARS coronavirus. A first step in understanding SARS pathogenesis. J Pathol 2004;203:631–637.
[13] Cheung OY, Chan JW, Ng CK, Koo CK. The spectrum of pathological changes in severe acute respiratory syndrome (SARS). Histopathology 2004;45:119–124.
[14] Chen J, Subbarao K. The immunobiology of SARS*. Annu Rev Immunol 2007;25:443–472.
[15] Chen G, Wu D, Guo W, Cao Y, Huang D, Wang H, et al. Clinical and immunologic features in severe and moderate coronavirus disease 2019. J Clin Invest 2020;130:2620–2629.

[16] Henrion J, Schapira M, Luwaert R, Colin L, Delannoy A, Heller FR. Hypoxic hepatitis: clinical and hemodynamic study in 142 consecutive cases. Medicine (Baltimore) 2003;82:392–406.
[17] Seeto RK, Fenn B, Rockey DC. Ischemic hepatitis: clinical presentation and pathogenesis. Am J Med 2000;109:109–113.
[18] Bessone F, Dirchwolf M, Rodil MA, Razori MV, Roma MG. Review article: drug-induced liver injury in the context of nonalcoholic fatty liver disease - a physiopathological and clinical integrated view. Aliment Pharmacol Ther 2018;48:892–913.
[19] Gordon A, McLean CA, Pedersen JS, Bailey MJ, Roberts SK. Hepatic steatosis in chronic hepatitis B and C: predictors, distribution and effect on fibrosis. J Hepatol 2005;43:38–44.
[20] Nishida N, Chiba T, Ohtani M, Yoshioka N. Sudden unexpected death of a 17-year-old male infected with the influenza virus. Leg Med (Tokyo) 2005;7:51–57.